

SOIL MOISTURE MAPPING FROM ASAR IMAGERY FOR THE FLUMENDOSA AND MEUSE RIVER BASINS

C. Paniconi⁽¹⁾, P. A. Troch⁽²⁾, M. Mancini⁽³⁾, M. A. Dessena⁽⁴⁾

⁽¹⁾*Centro di Ricerca, Sviluppo e Studi Superiori in Sardegna (CRS4)
6° Strada O., Z.I. Macchiareddu, C.P. 94
09010 Uta (Cagliari) - Italy
email: cspanico@crs4.it*

⁽²⁾*Wageningen University and Research Center
Nieuwe Kanaal, 11
6709 PA Wageningen - The Netherlands
email: peter.troch@users.whh.wau.nl*

⁽³⁾*Politecnico di Milano
Piazza Leonardo da Vinci, 32
20133 Milano - Italy
email: mmancini@idra1.iar.polimi.it*

⁽⁴⁾*Ente Autonomo Flumendosa
Viale Elmas, 116
09123 Cagliari - Italy
email: paobotti@tin.it*

INTRODUCTION

Soil moisture monitoring and the characterization of the spatial and temporal variability of this hydrologic parameter at scales from small catchments to large river basins continues to receive much attention, reflecting its critical role in subsurface – land surface – atmosphere interactions and its importance to drought analysis, crop yield forecasting, irrigation planning, flood protection, and forest fire prevention [1, 2, 3, 4].

We will describe the objectives and methodologies of an Envisat project that will aim to produce maps of seasonal soil moisture patterns at the regional scale based on ASAR imagery. The work will be carried out for two river basins that have significantly different climatic, geologic, and land use characteristics: the Flumendosa basin in Sardinia (Italy) and the larger Meuse basin that drains a good part of Belgium and the Netherlands as well as portions of France, Germany, and Luxembourg. High resolution ASAR data will be acquired over selected catchment scale test sites within each of these study regions, whereas medium resolution images will be acquired over the entire river basin (or extended region in the case of the smaller basin). A statistical analysis of the information from the processed images at these two different scales will be used to develop an aggregation methodology to generate large scale soil moisture maps. Data assimilation techniques will also be developed for dynamically integrating the high resolution satellite data into catchment scale hydrological simulation models. The work being planned will be placed in the context of recent efforts at validating and applying SAR soil moisture data, which we will briefly review.

PREVIOUS WORK

Remote sensing offers the potential for frequent observation of soil moisture at basin and regional scales. A variety of infrared and microwave (both active and passive) sensors operating from laboratory, aircraft, and satellite platforms have been tested for soil moisture retrieval, and the potentials and limitations of each of these remote sensing techniques are well documented [5, 6, 7].

Whereas recent studies have successfully demonstrated the use of infrared, passive microwave, and non-SAR sensors to obtain soil moisture information [8, 9, 10], the potential of active microwave remote sensing based on synthetic aperture radar instruments remains largely unrealized. The main advantage of radar is that it provides observations at a high spatial resolution of tens of meters compared to tens of kilometers for passive satellite instruments such as radiometers or non-SAR active instruments such as scatterometers. The main difficulty with SAR imagery is that soil moisture, surface roughness, and vegetation cover all have an important and nearly equal effect on radar backscatter. These interactions make retrieval of soil moisture possible only under particular conditions such as bare soil or surfaces with low vegetation density [11, 12, 13, 14, 15, 16].

Soil Moisture Mapping

It should be possible to separate the vegetation, topography, and soil moisture effects on radar response using multifrequency and/or multipolarization measurements [17], but currently operational satellites are not equipped with sensors that provide such data. A related concept that can be applied to existing satellite imagery is multitemporal analysis. Although on its own it will not produce direct or absolute measurements, multitemporal analysis could be useful for deriving wetness indices and for monitoring temporal changes or elucidating spatial patterns in soil moisture. In addition, such detection techniques may provide estimates or maps of other hydrologic features or parameters that are sensitive to or affect the spatial distribution of soil moisture, such as the extent of floodplains and recharge/discharge areas, soil texture and hydraulic characteristics [18, 19], the time to onset of soil limited (stage-two) evaporation [20], and the dynamics of variable source areas.

SAR mapping of the saturated surfaces of a watershed from variable source areas and other mechanisms relies on the fact that when ponding occurs the radar signal drops due to specular reflection, thus giving rise to a threshold behavior in backscattering response. However, applying a threshold on the backscattering coefficient is not successful in delineating saturated areas since the choice of an absolute threshold cannot take account of the various surface characteristics that influence the backscatter. In cases where vegetation and topographic effects are less prominent than soil moisture effects, simple statistical techniques, such as calculating the standard deviation for each pixel over a period of time, are able to reveal soil moisture or saturation patterns [21, 22]. Since such cases are atypical and cannot normally be identified a priori, a more robust technique is sought.

A multitemporal analysis based on the principal components transformation has shown that the soil moisture information in SAR images can be separated from other physical factors that influence the radar response [23]. The principal component analysis (PCA) was applied to a winter-time sequence of eight ERS (European Remote Sensing) satellite images acquired over the Zwalm catchment in Belgium. In the images constructed from the first three principal components, effects due to local incidence angle (topography), land cover (forests and urban areas), and soil moisture are isolated. The latter image displays spatial patterns that are consistent with soil moisture behavior expected from the runoff and drainage response of the basin to rainfall events.

The Zwalm catchment study site is situated about 20 km south of Gent in Belgium. It is a 5th Strahler-order basin with a total drainage area of 114 km² and a drainage density of 1.55 km/km². Rolling hills and mild slopes, with a maximum elevation difference of 150 m, characterize the topography. Land use is mainly arable crop farming and permanent pasture, while the south of the catchment is partly forested. The degree of urbanization is about 10%, and is mainly clustered in three small towns. The soil type in the catchment is predominantly sandy loam with minor isolated patches of sand and clay. The climatic regime is humid temperate with a mean annual rainfall of 775 mm distributed almost uniformly over the year and a mean annual pan evapotranspiration of 450 mm.

A sequence of 4 pairs of tandem ERS-1/2 SAR images (C-band, 5.3 GHz, VV polarization, spatial resolution 30 × 30 m) was acquired over the Zwalm catchment during the winter period of 1995-1996. Winter-time images were selected for

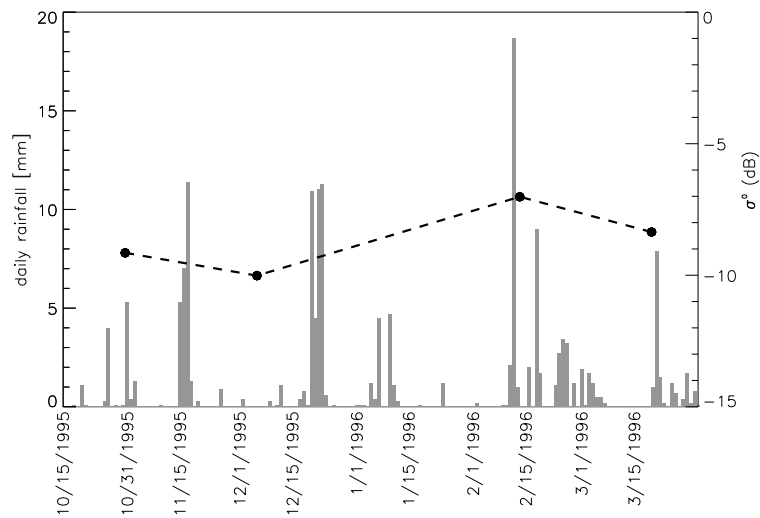


Figure 1: Daily rainfall for the 1995-1996 winter period. Also indicated by the dashed line and right-hand scale is the average radar backscatter σ^0 for the catchment calculated for each tandem pair of ERS-1/2 images.

the study in order to minimize soil roughness and vegetation changes. Fig. 1 shows the daily rainfall for the study period together and the average backscattering coefficient over the whole catchment calculated from the eight SAR images. From this figure it is apparent that the scene information is strongly affected by the rainfall episodes.

Pre-processing of the SAR images involved georeferencing using 15 ground control points and an existing SPOT image of the same region, calibration based on a procedure described in [24], and speckle reduction using the gamma MAP filter [25].

The principal components transformation is a standard tool in image enhancement, image compression, and classification [26, 27, 28] that linearly transforms multispectral or multidimensional data into a new coordinate system in which the data can be represented without correlation. The new coordinate axes are orthogonal to each other and point in the direction of decreasing order of the variances, so that the first principal component contains the largest percentage of the total variance (hence the maximum or dominant information), the second component the second largest percentage, and so on. Images transformed by PCA may make evident features that are not discernable in the original data — local details in multispectral images, changes and trends in multitemporal data — that typically show up in the intermediate principal components.

Applying PCA to the eight SAR images leads to the separation of the information contained in the images into several components that can be attributed to different factors influencing the backscatter. In our analysis the first principal component accounts for 76.6% of the total variance, the second component for 6.6%, the third for 5.9%, and each of the remaining PCs for less than 4%. Comparing the first component image with a mapping of local incidence angles computed from the digital elevation model of the catchment, it is apparent that topographic effects are responsible for the largest contribution to the total variance in the sequence of SAR images and dominate the backscattering signal.

The second principal component image displays a strong spatial organization, with the highest values grouped along the drainage network of the catchment, and corresponds closely with a soil drainage map for the catchment (Fig. 2). Poorly-drained soils tend to occur in the valley regions of the catchment and correspond well with the areas with high second PC values. This suggests a radar response, brought out in the second principal component, to the soil moisture patterns that result from the drainage characteristics of the basin. These patterns are not attributable to any single event, but reflect the overall response of the soil to the rainfall and interstorm periods spanned by the images.

The third principal component showed the influence of land cover and land use, matching closely the forested and urbanized areas seen from a Landsat image. The fourth and subsequent principal components accounted for a smaller fraction of the total variance in the sequence of SAR images, and they did not seem to reveal significant geophysical features.

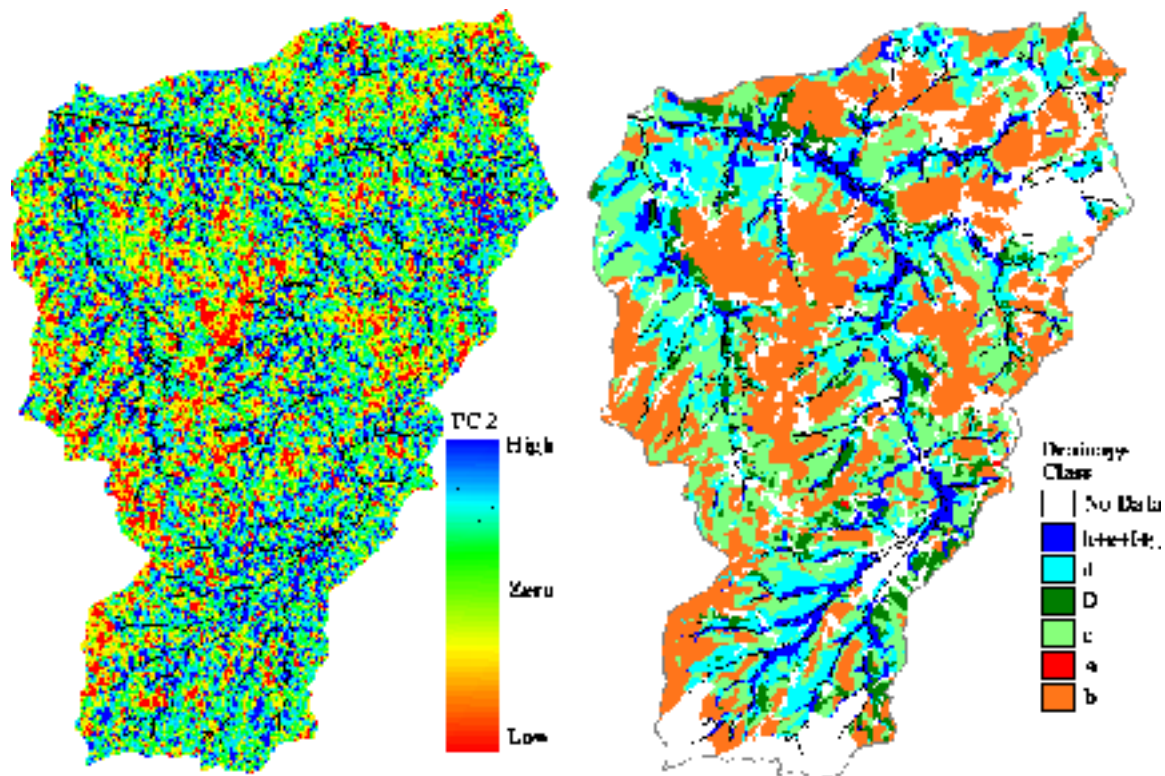


Figure 2: Second principal component image (left) and the drainage map for the catchment (right).

These PCs are characterized mostly by noise (including speckle).

This application of PCA to SAR images of the Zwalm images suggests that active microwave remote sensing is able to detect or map changes in surface soil moisture at basin scales. To test and improve the methodology, application to other basins and non-winter sets of images is needed.

WORK PLANNED

The objective of the work being planned is to produce maps of seasonal soil moisture patterns at the regional scale based on medium resolution ASAR imagery. The PCA-based mapping already demonstrated for a small catchment will be extended to larger basins using statistical aggregation of high resolution images to medium resolution. High resolution data will be acquired over a selected basin scale test site within each of the Flumendosa and Meuse basins, whereas medium resolution images will be acquired over the whole basin. A statistical analysis of the information from the processed images at these two different scales will be used to develop an aggregation methodology to generate large scale soil moisture maps. The results expected from the project are:

- Validation of the multitemporal analysis technique previously applied to a single series of high resolution (ERS-1/2) images;
- Extension of this soil moisture mapping methodology to regional scales and medium resolution imagery;
- Demonstration of the potential to produce seasonal soil moisture maps at catchment and regional scales under different physiographic conditions;
- Implementation and testing of data assimilation techniques for dynamically integrating soil moisture observation data into catchment scale hydrological simulation models.

The work will involve the following phases over a 4–5 year period:

1. Preparation

- Set-up of GIS database for the two regions;
- Acquisition of auxiliary satellite data (Landsat and/or SPOT);
- Acquisition and processing of ERS-2 SAR PRI for sites with no prior SAR data.

2. Data acquisition

- Meuse: two winter series of ASAR high and medium resolution images;
- Flumendosa: one year series of ASAR high and medium resolution images.

3. Analysis

- Image processing (including georeferencing and speckle filtering);
- Mosaicing;
- Multitemporal analysis of both high and medium resolution data;
- Development and validation of aggregation methodology.

4. Assimilation

- Implementation and testing of simple sub-optimal data assimilation methods in a detailed physically-based hydrologic model;
- Assessment of more sophisticated optimal data assimilation techniques;
- Application to estimation of soil moisture profiles from surface observation data.

5. Reporting

- Preliminary reporting at end of each phase;
- Reporting at ESA and other symposia and workshops;
- Final reporting.

Description of the Test Sites

Meuse. The Meuse river basin, one of the major watersheds in western Europe, has a total length of 870 km from its source to the Hollands Diep and a drainage area of about 33 000 km². 28% of the catchment area is situated in France, 41% in Belgium, 12% in Germany, 19% in The Netherlands, and a small portion in Luxembourg. The climate is influenced by proximity to the Atlantic Ocean and is characterized by rainfall throughout the year rather than distinct wet and dry seasons. The streamflow is very variable; for instance at Borgharen, downstream of Maastricht, the average streamflow is 230 m³/s but it may be as low as 25 m³/s and as high as 3120 m³/s (Dec 1993). Hydrographically the Meuse basin can be subdivided into three main parts, the Meuse Lorraine, Meuse Ardennaise, and lower reaches.

The Meuse Lorraine is a rural area with low population density, and comprises the upper reaches in France, from the source at Pouilly-en-Bassigny, to the confluence with the river Chiers near Sedan. This part of the catchment is lengthy and narrow, the slopes are gentle, and the main streambed is wide. During high discharge events the riverbed floods, and water velocity is low.

The Meuse Ardennaise comprises the central reaches, from Sedan to the Belgian-Dutch border between Visé and Eijsden. The main tributaries are the Viroin, the Semois, the Lesse, the Sambre, and the Ourthe. Due to the orography, precipitation in this area, at > 1000 mm/yr, is higher than in the rest of the basin. The slopes are rocky and steep, and the streambed is narrow. The poor permeability of most of the catchment area and the steep slope of the Meuse and most of its tributaries contribute to a fast flow response to rainfall. The contribution of the area to flood waves is great, while its contribution to low flows is small. Almost the entire stretch of the river is navigable, and water levels are maintained by many weirs.

The lower reaches of the Meuse correspond to the Dutch section of the river and can be further split into the stretches from Eijsden to Maasbracht and from Maasbracht to the confluence with the river Rhine in the Hollands Diep. In the

upper part, called Grensmaas or Gemeenschappelijke Maas along the Belgian-Dutch border, the slope is relatively steep and the river has no dikes and for the most part no weirs. Shipping uses the parallel Juliana Channel. The part of the river downstream of Maasbracht is provided with weirs for navigation. The main tributaries are the Roer (Ruhr) and the Niers. The Roer contains reservoirs and so discharge is minimal. From Boxmeer the river is a typical lowland stream, with dikes and flood plains. Downstream of Lith the river is not canalized and is subject to tidal influences (Getijdemaas). Flooding problems arise in particular in the section without dikes. During the flooding of 1993, 13 000 people were evacuated, and 200 000 in the 1995 floods.

Geomorphological, hydrological, and meteorological data available for the Meuse basin includes: 1 km and 75 m resolution DEMs; 100 m resolution CORINE land cover (44 classes); European Soils Database (1:1.000.000 scale) containing soil texture, depth to impermeable layer, rooting depth, and parent material; HYPRES soil physical database (transfer functions); GISCO database with European rivers; Rijkswaterstaat map of the river and tributaries; daily and hourly precipitation; minimum and maximum daily temperature; actual vapour pressure, sunshine duration, cloud cover, and windspeed; daily discharges at many gauging stations.

Flumendosa. The Flumendosa river basin has a drainage area of 1800 km² and is located in the central-eastern part of the island of Sardinia in Italy. It is bounded in the north and northeast by the Gennargentu and Ogliastra mountains and in the west by Miocene formations of gentler relief. The basin outlets to the sea on the southeastern coastal plain around the towns of Muravera, San Vito, and Villaputzu. The northern more mountainous part of the basin occupies about 1180 km².

Mean annual rainfall for the entire basin is about 860 mm, which is higher than the mean annual rainfall of 775 mm over all of Sardinia. The rainiest months are November and December, and the most arid month is July. Precipitation patterns over the basin are non-uniform and highly correlated to topography, with 650 mm average rainfall below 200 m.a.s.l. and 1285 mm above 1000 m. The highest peak in the basin (and in Sardinia) is Bruncu Spina at 1829 m. The climate of the basin can be classified as humid Mediterranean above 500 m elevation and as sub-humid Mediterranean below 500 m.

The dominant geological formations within the Flumendosa basin run from northeast to southwest and are characterized as carbonate-schist, metavolcanic, and metacalcareous complexes. During the Quaternary period intense erosional processes occurred, resulting in alluvial deposits which can be found throughout the basin. Geomorphologically, the basin varies from canyon formations and meandering channels in the mountainous portion to gentle hills and wide valleys in the more southern parts.

The soils in the basin are generally of modest thickness and the microrelief frequently rocky. Soil humidity, as with rainfall, is highly spatially and temporally variably, and in the driest months the soil wetness in large parts of the basin reaches residual values. The vegetation throughout the basin has been notably altered by human activities, with many areas converted to pasture. The most intense agricultural activities are in the southcentral and southeastern parts of the basin, with cultivation of grains, vines, and citrus orchards making up the most common agricultural land uses. Many areas have been reforested, and in the northern parts of the basin natural vegetation cover is still present and is a mixture of bare soil, grassland, shrubs, and forests.

Geomorphological, hydrological, and meteorological data available for the Flumendosa basin includes: 8 meteorological stations for rainfall and other climatic variables; 10 automatic hydrometric stations for streamflow measurements; regular (weekly or fortnightly) water quality sampling; data regarding runoff, sediment transport, and erosion processes on selected small subcatchments; topographic maps at 1:25.000 and 1:50.000 scales; aerial photographs at 1:33.000 scale; digital thematic maps at 1:25.000 scale of lithology, morphology, pedology, soil classification for irrigability, land use and land cover, land units, erosion classes, and population; digital elevation model at 1:25.000 scale in UTM and Gauss-Boaga coordinates at 40 m resolution; Landsat TM and IRS-1C satellite images.

ASAR data. ASAR Wide Swath Medium Resolution imagery will be collected over the entire territory of the Meuse and Flumendosa basins. Within each of these two regions, ASAR Image Mode Precision Image data will be acquired over selected basin scale test sites. For the Meuse basin and sub-basins, multitemporal analysis of the radar images will be used to study seasonal soil moisture fluctuations in an attempt to quantify the temporal variability of surface soil moisture content with the aim of mapping variable source areas. The variable source area concept, now widely accepted to explain storm runoff production in humid regions, describes how the yielding proportion of a watershed expands and shrinks

depending on rainfall amount and antecedent wetness of the soil [29]. A major feature of variable source areas is that the area over which return flow and direct precipitation are generated varies seasonally and throughout a storm.

For the Flumendosa basin, the soil moisture patterns expected to be extracted from the SAR signal will not necessarily coincide with the drainage network, as in the case for the more humid Meuse basin, but will probably show less correlation in space and will be determined more by local soil and geological characteristics of the basin. Also, the influence of vegetation growth on the total SAR signal is expected to be less dominant, since vegetation is mainly shrubland and bushes which are permanently present. These hydrological, geomorphological and ecological characteristics constitute an important complement to the corresponding features of the Meuse basin, and will provide an opportunity to demonstrate the SAR analysis methodology under different physiographic conditions. For this area ASAR data for a complete hydrological year will be collected, to be analyzed both as a single annual sequence of images and as separate summer and winter sequences, allowing comparison of inter-seasonal soil moisture behavior.

Methodology

Basic image processing. Basic image processing to be performed involves calibration with respect to a common calibration factor (in the case of images generated by different PAFs), georeferencing, mosaicing, and speckle filtering. Soil moisture patterns can be extracted from these pre-processed data by means of multitemporal analysis.

Multitemporal analysis. The principal components transformation will be used. This will involve calculating the eigenvalues and eigenvectors of the cross-covariance matrix of a series of images. Since the eigenvalues are the diagonal elements of the covariance matrix in the transformed coordinate system, they express the variance attributable to each principal component. The principal components are the projection coefficients on the principal axes of the new coordinate system.

Aggregation. The final step in the processing and analysis of the SAR imagery is the application of an appropriate aggregation methodology to conserve spatial patterns, detected by the high resolution data, in the medium resolution data products. Aggregating soil moisture information from high resolution SAR imagery to medium resolution will involve the determination of the statistical characteristics (variances and covariances) of delineated hydrological units (such as contributing areas in the humid catchments), and to correct the processing results based on medium resolution imagery accordingly. The statistical correction will be based on averaging techniques that take into account the correlation structure of the spatial data.

Data Assimilation

Continued progress in our scientific understanding of hydrological processes at the catchment scale relies on making the best possible use of advanced simulation models and the large amounts of environmental data that are increasingly being made available. A wide variety of distributed hydrological models has been developed over the past decades, with the common feature of being able to incorporate the spatial distribution of various inputs and boundary conditions (topography, vegetation, land use, soil characteristics, rainfall, evaporation) and to produce spatially detailed outputs such as soil moisture fields, water table positions, groundwater fluxes, and surface saturation patterns. A major factor contributing to the popularity of the distributed modeling approach is the availability of digital terrain data, and GIS-based algorithms for extraction of hydrologically relevant information from this data. One of the major problems plaguing distributed modeling is parameter identifiability, owing to a mismatch between model complexity and the level of data which is available to parameterize, initialize, and calibrate models, and to uncertainty and error in both models and observation data.

New data sources, both in situ and remote, for observation of hydrological processes can alleviate some of the problems facing the validation and operational use of hydrological models. In situ and remote measurement techniques are complementary, the one offering high temporal detail and the other fine spatial resolution. The final phases of the work being planned will investigate the combined use of models and remotely sensed soil moisture data, in particular for inferring

soil moisture information for the deeper layers of the soil profile, beyond the 5–20 centimeters directly detectable by remote sensors [30, 31, 32, 33].

In general terms, geophysical data assimilation is a quantitative, objective method to infer the state of the earth-atmosphere-ocean system from heterogeneous, irregularly distributed, and temporally inconsistent observational data with differing accuracies [34, 35, 36]. It represents a formal methodology to integrate these data with simulation models to provide physically consistent estimates of spatially distributed environmental variables, providing at the same time more reliable information about prediction uncertainty in model forecasts. In operational systems where observation data is available on a routine basis at regular intervals, data assimilation is an important tool in assessing data quality, identifying for instance any biases or systematic errors in satellite-based sensors. Data assimilation is by now routinely used in research and operational meteorology, although many scientific challenges remain for improving and extending existing methodologies. More recently, data assimilation is being introduced in the oceanographical and hydrological sciences, owing to the trend towards better and more regular observation of a wide range of parameters of interest to the Earth sciences.

The physically-based catchment hydrologic model to be used, CATHY [37, 38, 39], is a coupled overland and subsurface flow model. The model simulates the dynamics of catchment flow processes in a consistent manner based on conservation principles, and so is a good candidate for data assimilation. The model readily produces detailed primary (pressure head) and derived (moisture content, integrated measures of soil water, surface saturations, water table positions, groundwater velocities, surface water fluxes) output fields at selected times that can be used for comparison against and integration with observation data in an assimilation context, in addition to hydrograph output (typically at the catchment outlet node) that gives the spatially integrated response of the basin to potential and actual atmospheric forcings and is the time series traditionally used for calibration of hydrologic models.

Some fairly simple data assimilation algorithms will be implemented as first trials for the CATHY model, in particular Newtonian relaxation or nudging [40]. More advanced methods that allow incorporation of model and data uncertainty in an optimal sense, such as variational data assimilation and extended Kalman filtering, will be explored in future work. The main concern at this stage is for a data assimilation formulation that can systematically combine information from different observation sources, both satellite and ground-based.

Nudging is a 4-dimensional data assimilation procedure in which model variables are driven towards observations. For the model equation

$$\frac{\partial s}{\partial t} = F(s) \quad (1)$$

an additional “forcing term” is introduced which is proportional to the difference between simulation and observation:

$$\frac{\partial s}{\partial t} = F(s) + GW(r, t)\epsilon(r)(s'_o - s) \quad (2)$$

where s'_o are the observations interpolated to the model grid, G determines the relative strength of the nudging term with respect to the physical forcing term, $W(r, t)$ is the weighting function, and $\epsilon \leq 1$ is a factor reflecting the accuracy of the observation data (1 for perfect data). The weighting function should reflect the spatial and temporal correlation structure of the state variable being assimilated. Expressing the weighting function as $W(r, t) = W(x, y)W(z)W(t)$, a commonly used functional form is:

$$W(x, y) = \frac{R^2 - D^2}{R^2 + D^2} \quad 0 \leq D \leq R \quad (3)$$

$$W(x, y) = 0 \quad D > R \quad (4)$$

$$W(z) = 1 - \frac{|z_o - z|}{R_z} \quad |z_o - z| \leq R_z \quad (5)$$

$$W(z) = 0 \quad |z_o - z| > R_z \quad (6)$$

$$W(t) = 1 \quad |t - t_o| < \frac{\tau}{4} \quad (7)$$

$$W(t) = \frac{(\tau - |t - t_o|)}{\tau/4} \quad \frac{\tau}{4} \leq |t - t_o| \leq \tau \quad (8)$$

$$W(t) = 0 \quad |t - t_o| > \tau \quad (9)$$

where R , R_z , and τ are the radii of influence and z_o and t_o are the vertical and temporal coordinates of the observation point.

Some important aspects of data assimilation, and of nudging in particular, to be investigated include:

- How does the nudging term impact mass conservation?;
- How does the nudging term (in particular the size of the G coefficient) impact numerical stability and convergence?;
- CPU aspects (especially with a view to implementation of more sophisticated or optimal data assimilation schemes);
- Differences in assimilation of remote sensing vs ground data.

Acknowledgements. This work has been funded by the Energy, Environment, and Sustainable Development Programme of the European Commission (contract EVK1-CT-1999-00022) and by the Sardinia Regional Authorities.

References

- [1] K. P. Georgakakos and O. W. Baumer. Measurement and utilization of on-site soil moisture data. *J. Hydrol.*, 184:131–152, 1996.
- [2] A. W. Western, R. B. Grayson, G. Blöschl, G. R. Willgoose, and T. A. McMahon. Observed spatial organization of soil moisture and its relation to terrain indices. *Water Resour. Res.*, 35(3):797–810, 1999.
- [3] A. Robock, K. Y. Vinnikov, G. Srinivasan, J. K. Entin, S. E. Hollinger, N. A. Speranskaya, S. Liu, and A. Namkhai. The Global Soil Moisture Data Bank. *Bull. Amer. Meteor. Soc.*, 81(6):1281–1299, 2000.
- [4] I. Rodríguez-Iturbe. Ecohydrology: A hydrologic perspective of climate-soil-vegetation dynamics. *Water Resour. Res.*, 36(1):3–9, 2000.
- [5] B. J. Choudhury. Multispectral satellite data in the context of land surface heat balance. *Rev. Geophys.*, 29(2):217–236, 1991.
- [6] K. Blyth. The use of microwave remote sensing to improve spatial parameterization of hydrological models. *J. Hydrol.*, 152:103–129, 1993.
- [7] E. T. Engman. Recent advances in remote sensing in hydrology. In R. A. Pielke Sr. and R. M. Vogel, editors, *U.S. National Report to International Union of Geodesy and Geophysics 1991–1994: Contributions in Hydrology*, pages 967–975. American Geophysical Union, Washington, DC, 1995.
- [8] W. J. Capehart and T. N. Carlson. Decoupling of surface and near-surface soil water content: A remote sensing perspective. *Water Resour. Res.*, 33(6):1383–1395, 1997.
- [9] T. J. Jackson. Soil moisture estimation using special satellite microwave/imager satellite data over a grassland region. *Water Resour. Res.*, 33(6):1475–1484, 1997.
- [10] W. Wagner, M. Borgeaud, and J. Noll. Soil moisture mapping with the ERS scatterometer. *Earth Observation Quarterly*, 54:4–7, December 1996.
- [11] F. T. Ulaby, R. K. Moore, and A. K. Fung. *Microwave Remote Sensing, Active and Passive, Vol. 2*. Artech House, 1982.
- [12] A.-L. Cognard, C. Loumagne, M. Normand, P. Olivier, C. Ottlé, D. Vidal-Madjar, S. Louahala, and A. Vidal. Evaluation of the ERS 1/synthetic aperture radar capacity to estimate surface soil moisture: Two-year results over the Naizin watershed. *Water Resour. Res.*, 31(4):975–982, 1995.
- [13] E. Altese, O. Bolognani, M. Mancini, and P. A. Troch. Retrieving soil moisture over bare soil from ERS 1 synthetic aperture radar data: Sensitivity analysis based on a theoretical surface scattering model and field data. *Water Resour. Res.*, 32(3):653–661, 1996.

- [14] E. E. Sano, A. R. Huete, D. Trouffleau, M. S. Moran, and A. Vidal. Relation between ERS-1 synthetic aperture radar data and measurements of surface roughness and moisture content of rocky soils in a semiarid rangeland. *Water Resour. Res.*, 34(6):1491–1498, 1998.
- [15] G. F. Biftu and T. Y. Gan. Retrieving near-surface soil moisture from Radarsat SAR data. *Water Resour. Res.*, 35(5):1569–1579, 1999.
- [16] M. Mancini, R. Hoeben, and P. A. Troch. Multifrequency radar observations of bare surface soil moisture content: A laboratory experiment. *Water Resour. Res.*, 35(6):1827–1838, 1999.
- [17] F. T. Ulaby, P. C. Dubois, and J. van Zyl. Radar mapping of surface soil moisture. *J. Hydrol.*, 184:57–84, 1996.
- [18] K. J. Hollenbeck, T. J. Schmugge, G. M. Hornberger, and J. R. Wang. Identifying soil hydraulic heterogeneity by detection of relative change in passive microwave remote sensing observations. *Water Resour. Res.*, 32(1):139–148, 1996.
- [19] N. M. Mattikalli, E. T. Engman, L. R. Ahuja, and T. J. Jackson. A GIS for spatial and temporal monitoring of microwave remotely sensed soil moisture and estimation of soil properties. In *Application of Geographic Information Systems in Hydrology and Water Resources Management*, pages 621–628, IAHS Press, Institute of Hydrology, Wallingford, UK, 1996.
- [20] G. D. Salvucci. Soil and moisture independent estimation of stage-two evaporation from potential evaporation and albedo or surface temperature. *Water Resour. Res.*, 33(1):111–122, 1997.
- [21] E. J. M. Rignot and J. van Zyl. Change detection techniques for ERS-1 SAR data. *IEEE Trans. Geosc. Rem. Sens.*, 31(4):896–906, 1993.
- [22] P. A. Troch, N. E. C. Verhoest, P. Gineste, C. Paniconi, and P. Mérot. Variable source areas, soil moisture and active microwave observations at Zwalmbeek and Coët-Dan. In R. Grayson and G. Blöschl, editors, *Spatial Patterns in Catchment Hydrology: Observations and Modelling*. Cambridge University Press, Cambridge, UK (in press), 2000.
- [23] N. E. C. Verhoest, P. A. Troch, C. Paniconi, and F. P. De Troch. Mapping basin scale variable source areas from multitemporal remotely sensed observations of soil moisture behavior. *Water Resour. Res.*, 34(12):3235–3244, 1998.
- [24] H. Laur, P. Bally, P. Meadows, J. Sanchez, B. Schaettler, and E. Lopinto. ERS SAR calibration: derivation of backscattering coefficient σ^0 in ESA ERS SAR PRI products. Technical report, European Space Agency, Frascati, Italy, 1997.
- [25] A. Lopes, E. Nezry, R. Touzi, and H. Laur. Structure detection and statistical adaptive speckle filtering in SAR images. *Int. J. Rem. Sens.*, 14(9):1735–1758, 1993.
- [26] J. A. Richards. *Remote Sensing Digital Image Analysis*. Springer-Verlag, New York, NY, 1986.
- [27] A. Singh. Digital change detection techniques using remotely-sensed data. *Int. J. Remote Sensing*, 10(6):989–1003, 1989.
- [28] J.-S. Lee and K. Hoppel. Principal components transformation of multifrequency polarimetric SAR imagery. *IEEE Trans. Geosci. Remote Sensing*, 30(4):686–696, 1992.
- [29] J. D. Hewlett and A. R. Hibbert. Factors affecting the response of small watersheds to precipitation in humid areas. In W. S. Sooper and H. W. Lull, editors, *Forest Hydrology*, pages 275–290, Pergamon Press, Oxford, UK, 1967.
- [30] D. Entekhabi, H. Nakamura, and E. G. Njoku. Solving the inverse problem for soil moisture and temperature profiles by sequential assimilation of multifrequency remotely sensed observations. *IEEE Trans. Geosci. Remote Sensing*, 32(2):438–447, 1994.
- [31] P. R. Houser, W. J. Shuttleworth, J. S. Famiglietti, H. V. Gupta, K. H. Syed, and D. C. Goodrich. Integration of soil moisture remote sensing and hydrologic modeling using data assimilation. *Water Resour. Res.*, 34(12):3405–3420, 1998.

- [32] R. H. Reichle, D. McLaughlin, and D. Entekhabi. Variational data assimilation of soil moisture and temperature from remote sensing observations. In *ModelCARE 99 Proceedings of the International Conference on Calibration and Reliability in Groundwater Modeling*, pages 437–442, ETH Zurich, Zurich, Switzerland, 1999.
- [33] R. Hoeben and P. A. Troch. Assimilation of active microwave observation data for soil moisture profile estimation. *Water Resour. Res.*, 2000 (to appear).
- [34] R. Daley. *Atmospheric Data Analysis*. Cambridge University Press, Cambridge, UK, 1991.
- [35] U. S. National Research Council. *Four-Dimensional Model Assimilation of Data: A Strategy for the Earth System Sciences*. National Academy Press, Washington, DC, 1991.
- [36] D. McLaughlin. Recent developments in hydrologic data assimilation. In R. A. Pielke Sr. and R. M. Vogel, editors, *U.S. National Report to International Union of Geodesy and Geophysics 1991–1994: Contributions in Hydrology*, pages 977–984. American Geophysical Union, Washington, DC, 1995.
- [37] C. Paniconi and E. F. Wood. A detailed model for simulation of catchment scale subsurface hydrologic processes. *Water Resour. Res.*, 29(6):1601–1620, 1993.
- [38] S. Orlandini and R. Rosso. Diffusion wave modeling of distributed catchment dynamics. *J. Hydrol. Engrg., ASCE*, 1(3):103–113, 1996.
- [39] A. C. Bixio, S. Orlandini, C. Paniconi, and M. Putti. Physically-based distributed model for coupled surface runoff and subsurface flow simulation at the catchment scale. In *Computational Methods in Water Resources, Vol. 2*, pages 1115–1122, Balkema, Rotterdam, The Netherlands, 2000.
- [40] M. Marrocu and C. Paniconi. Assessment and formulation of data assimilation techniques for a 3D Richards equation-based hydrological model. Technical Report CRS4 Technical Report, Center for Advanced Studies, Research and Development in Sardinia, Cagliari, Italy, 2000.